

# System size dependence of particle-ratio fluctuations in Pb+Pb collisions at 158A GeV

T. Anticic<sup>22</sup>, B. Baatar<sup>8</sup>, D. Barna<sup>4</sup>, J. Bartke<sup>6</sup>, H. Beck<sup>9</sup>, L. Betev<sup>10</sup>, H. Białkowska<sup>19</sup>, C. Blume<sup>9</sup>, M. Bogusz<sup>21</sup>, B. Boimska<sup>19</sup>, J. Book<sup>9</sup>, M. Botje<sup>1</sup>, P. Bunčić<sup>10</sup>, T. Cetner<sup>21</sup>, P. Christakoglou<sup>1</sup>, P. Chung<sup>18</sup>, O. Chvála<sup>14</sup>, J.G. Cramer<sup>15</sup>, V. Eckardt<sup>13</sup>, Z. Fodor<sup>4</sup>, P. Foka<sup>7</sup>, V. Friese<sup>7</sup>, M. Gaździcki<sup>9,11</sup>, K. Grebieszko<sup>21</sup>, C. Höhne<sup>7</sup>, K. Kadija<sup>22</sup>, A. Karev<sup>10</sup>, V.I. Kolesnikov<sup>8</sup>, T. Kollegger<sup>9</sup>, M. Kowalski<sup>6</sup>, D. Kresan<sup>7</sup>, A. László<sup>4</sup>, R. Lacey<sup>18</sup>, M. van Leeuwen<sup>1</sup>, M. Maćkowiak-Pawłowska<sup>21</sup>, M. Makariev<sup>17</sup>, A.I. Malakhov<sup>8</sup>, M. Mateev<sup>16</sup>, G.L. Melkumov<sup>8</sup>, M. Mitrovski<sup>9</sup>, St. Mrówczyński<sup>11</sup>, V. Nikolic<sup>22</sup>, G. Pála<sup>4</sup>, A.D. Panagiotou<sup>2</sup>, W. Peryt<sup>21</sup>, J. Pluta<sup>21</sup>, D. Prindle<sup>15</sup>, F. Pühlhofer<sup>12</sup>, R. Renfordt<sup>9</sup>, C. Roland<sup>5</sup>, G. Roland<sup>5</sup>, M. Rybczyński<sup>11</sup>, A. Rybicki<sup>6</sup>, A. Sandoval<sup>7</sup>, N. Schmitz<sup>13</sup>, T. Schuster<sup>9</sup>, P. Seyboth<sup>13</sup>, F. Siklér<sup>4</sup>, E. Skrzypczak<sup>20</sup>, M. Słodkowski<sup>21</sup>, G. Stefanek<sup>11</sup>, R. Stock<sup>9</sup>, H. Ströbele<sup>9</sup>, T. Susa<sup>22</sup>, M. Szuba<sup>21</sup>, M. Utvić<sup>9</sup>, D. Varga<sup>3</sup>, M. Vassiliou<sup>2</sup>, G.I. Veres<sup>4</sup>, G. Vesztergombi<sup>4</sup>, D. Vranić<sup>7</sup>, Z. Włodarczyk<sup>11</sup>, A. Wojtaszek-Szwarc<sup>11</sup>

<sup>1</sup> *NIKHEF, Amsterdam, Netherlands.*

<sup>2</sup> *Department of Physics,  
University of Athens, Athens, Greece.*

<sup>3</sup> *Eötvös Loránt University,  
Budapest, Hungary*

<sup>4</sup> *Wigner Research Center for Physics,  
Hungarian Academy of Sciences,  
Budapest, Hungary.*

<sup>5</sup> *MIT, Cambridge, Massachusetts, USA.*

<sup>6</sup> *H. Niewodniczański Institute of Nuclear Physics,  
Polish Academy of Sciences,  
Cracow, Poland.*

<sup>7</sup> *GSI Helmholtzzentrum für Schwerionenforschung GmbH,  
Darmstadt, Germany.*

<sup>8</sup> *Joint Institute for Nuclear Research,  
Dubna, Russia.*

- <sup>9</sup> *Fachbereich Physik der Universität,  
Frankfurt, Germany.*
- <sup>10</sup> *CERN, Geneva, Switzerland.*
- <sup>11</sup> *Institute of Physics,  
Jan Kochanowski University, Kielce, Poland.*
- <sup>12</sup> *Fachbereich Physik der Universität,  
Marburg, Germany.*
- <sup>13</sup> *Max-Planck-Institut für Physik,  
Munich, Germany.*
- <sup>14</sup> *Institute of Particle and Nuclear Physics,  
Charles University,  
Prague, Czech Republic.*
- <sup>15</sup> *Nuclear Physics Laboratory,  
University of Washington,  
Seattle, Washington, USA.*
- <sup>16</sup> *Atomic Physics Department,  
Sofia University St. Kliment Ohridski,  
Sofia, Bulgaria.*
- <sup>17</sup> *Institute for Nuclear Research and Nuclear Energy,  
BAS, Sofia, Bulgaria.*
- <sup>18</sup> *Department of Chemistry,  
Stony Brook University (SUNYSB),  
Stony Brook, New York, USA.*
- <sup>19</sup> *Institute for Nuclear Studies,  
Warsaw, Poland.*
- <sup>20</sup> *Institute for Experimental Physics,  
University of Warsaw, Warsaw, Poland.*
- <sup>21</sup> *Faculty of Physics,  
Warsaw University of Technology,  
Warsaw, Poland.*

<sup>22</sup> *Rudjer Boskovic Institute,  
Zagreb, Croatia.*

(Dated: November 20, 2018)

## Abstract

New measurements by the NA49 experiment of the centrality dependence of event-by-event fluctuations of the particle yield ratios  $(K^+ + K^-)/(\pi^+ + \pi^-)$ ,  $(p + \bar{p})/(\pi^+ + \pi^-)$ , and  $(K^+ + K^-)/(p + \bar{p})$  are presented for Pb+Pb collisions at 158A GeV. The absolute values of the dynamical fluctuations of these ratios, quantified by the measure  $\sigma_{\text{dyn}}$ , increase by about a factor of two from central to semi-peripheral collisions. Multiplicity scaling scenarios are tested and found to apply for both the centrality and the previously published energy dependence of the  $(K^+ + K^-)/(\pi^+ + \pi^-)$  and  $(p + \bar{p})/(\pi^+ + \pi^-)$  ratio fluctuations. A description of the centrality and energy dependence of  $(K^+ + K^-)/(p + \bar{p})$  ratio fluctuations by a common scaling prescription is not possible since there is a sign change in the energy dependence.

## 1. INTRODUCTION

The search for structures in the QCD phase diagram, like the first order phase transition line from hadronic to partonic degrees of freedom or the critical endpoint, has become one of the main activities in current and future high-energy heavy-ion experiments [1–3]. The experimental signatures for these structures are the subject of ongoing discussions. Lattice QCD calculations show that in the co-existence region of hadronic and partonic degrees of freedom and in the vicinity of the critical endpoint event-by-event fluctuations of, for example, the strangeness-to-entropy ratio increase significantly [4–7]. Thus, a measurement of the energy dependence of a quantity sensitive to this ratio and an observation of a non-monotonic behavior may provide an indication of the location of the critical endpoint.

The NA49 experiment at the CERN Super Proton Synchrotron (SPS) analyzed the energy dependence of the ratio of inclusive  $K^+$  and  $\pi^+$  yields in central Pb + Pb collisions and observed a peak structure at beam energies around 30 - 40A GeV [8]. This motivated the analysis of event-by-event fluctuations of the  $(K^+ + K^-)/(\pi^+ + \pi^-)$  (denoted  $K/\pi$ ) [9],  $(p + \bar{p})/(\pi^+ + \pi^-)$  (denoted  $p/\pi$ ) [9] and  $(K^+ + K^-)/(p + \bar{p})$  (denoted  $K/p$ ) ratios [10] as function of the center-of-mass energy by means of the observable  $\sigma_{\text{dyn}}$  (see Eqs. 4,5 in section 3.4), which measures the dynamical contribution to the fluctuations of the event-by-event particle ratios. The  $K/\pi$  ratio fluctuations show a continuous increase towards lower collision energies, which is not reproduced by the UrQMD model [11], but obtained qualitatively by HSD model calculations [12]. The  $p/\pi$  ratio fluctuations as a function of the center-of-mass energy show negative values which indicate strong correlations. This observation is well reproduced by UrQMD model calculations and can be interpreted as the result of the production of nucleon resonances and their decays into pions and protons. The  $K/p$  ratio fluctuations exhibit a change of sign at  $\approx 30A$  GeV beam energy which is not well understood [10]. In view of the complex energy dependence of the fluctuations of the three particle ratios an additional study of their collision centrality dependence at the top SPS energy may help to clarify the interpretation. In particular, such an investigation may help to distinguish the contributions of the changing multiplicities and the genuine energy and collision volume dependence of the underlying correlations [13].

The STAR collaboration at the Relativistic Heavy Ion Collider (RHIC) also published results on particle-ratio fluctuations [14] employing the observable  $\nu_{\text{dyn}}$  (Eq. 7 in section

3.4). First results from a recent low energy scan in Au+Au collisions at  $\sqrt{s_{NN}} = 7.7$  GeV were presented at conferences [15] and show a different trend for the energy dependence of  $K/\pi$  and  $K/p$  fluctuations when compared using the equivalence relation between  $\nu_{\text{dyn}}$  and  $\sigma_{\text{dyn}}$  (see Eq. 7 in section 3.4). However, acceptance in both rapidity  $y$  and transverse momentum  $p_T$  as well as the selection procedure of collision centrality differ.

In this paper we address the dependence of event-by-event fluctuations of particle yield ratios on the centrality of Pb+Pb collisions in a fixed acceptance and at a beam energy of 158A GeV [16]. In section 2 we describe the experimental equipment, in section 3 the analysis procedures. Section 4 presents the experimental results and compares to various proposed multiplicity scaling schemes. A summary section 5 closes the paper.

## 2. THE NA49 EXPERIMENT

NA49 is a fixed target experiment [17] at the CERN SPS. The trajectories of charged particles are reconstructed in four large volume Time Projection Chambers (TPCs). Two of them (VTPCs) are placed inside of two superconducting dipole magnets for momentum determination. Two main TPCs (MTPCs) are located downstream of the magnets on both sides of the beam. The performance of the MTPCs is tuned for high precision measurements of the specific energy loss  $dE/dx$ , which is the basis for particle identification employed in this analysis (see section 3.3 and [18]). Except for the trigger and beam intensity the experimental conditions in this analysis are the same as described in [9]. The Pb beam had a typical intensity of  $10^4$  ions/s. The minimum bias trigger was derived from a He-Cerenkov counter placed behind the target. Only interactions which reduced the beam charge and thus the signal seen by this detector by at least 10%, were accepted. The trigger cross section thus defined is 5.7 b out of a total inelastic cross section of 7.15 b. The resulting ensemble of 174 K events was divided into centrality classes according to the energy measured in the Veto Calorimeter (VCAL) located 26 m downstream from the target.

### 3. DATA ANALYSIS

#### 3.1. Event, track selection and acceptance

In order to reject background interactions, a valid fit of an event vertex was required and a cut around the known target position was applied. The contamination by background events remaining after cuts on vertex position and quality amounts to less than 5% for the most peripheral collisions and is negligible for near-central collisions.

The useful acceptance for pions, kaons, and protons is constrained by the needs of particle identification. The separation power is highest for particles with large track lengths in the MTPCs which limits the analysis to the forward hemisphere in the center-of-mass frame. The coverage in the azimuthal angle  $\phi$  is a function of center-of-mass rapidity  $y$  and transverse momentum  $p_T$ . The loose and tight sets of track cuts used in the present analysis are given in Table I. These are identical to those employed previously in NA49 analyses of fluctuations [9]. The acceptance is not only determined by the track selection cuts. In addition, only phase space bins are used for which the inclusive  $dE/dx$  distributions have more than 3000 entries.

TABLE I: Loose and tight set of track cuts used in the analysis.

Cut description	Cut	
	Loose	Tight
$(dE/dx)/(dE/dx)_{\text{MIP}}$	$\leq 1.8$	$\leq 1.8$
Number of points in MTPC	$> 30$	$> 30$
Number of points in VTPC1	–	$> 10$
Number of points in VTPC2	–	$> 10$
Fraction of potential points found in MTPC	$\geq 50\%$	$\geq 50\%$
Number of entries required in phase space	$>3000$	$>3000$
bin for fit of inclusive $dE/dx$ distribution		
Cut in proton rapidity for $p_T \leq 0.2 \text{ GeV}/c$	$y < y_{\text{beam}} - 1$	$y < y_{\text{beam}} - 1$
Track fitted to primary vertex	–	yes
impact parameter $x$ -projection	–	$< 4 \text{ cm}$
impact parameter $y$ -projection	–	$< 0.5 \text{ cm}$

The acceptance after all selection cuts is shown in Fig. 1 for central colli-

sions. The range in  $p_T$  varies slightly depending on the number of events in the centrality bin.

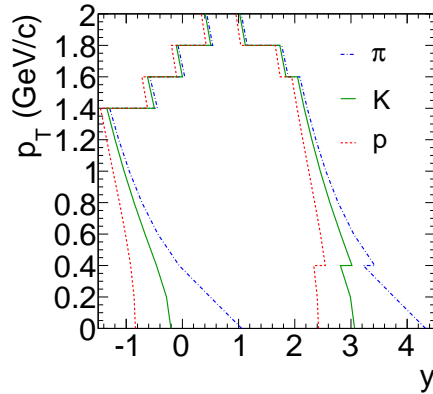


FIG. 1: (Color online) Acceptance in center-of-mass rapidity  $y$  and transverse momentum  $p_T$  for the most central Pb+Pb collisions at 158A GeV.

### 3.2. Collision centrality determination

The determination of the centrality of the collisions is based on the energy of forward going projectile spectators as measured in the VCAL. The distribution of the VCAL energy  $E_{\text{VETO}}$  together with the division into 5% bins of the total inelastic cross section is shown in Fig. 2.

The energy resolution of the VCAL measurement is dominated by two effects: the intrinsic energy resolution as given by the longitudinal sampling structure and by the non-uniformity of light collection efficiency. The overall resolution of the calorimeter was shown to follow [17]:

$$\frac{\sigma_E}{E} \approx \frac{2}{\sqrt{E}} \quad , \quad (1)$$

with  $E$  in units of GeV.

The choice of 5% centrality bin size is motivated by the energy resolution of VCAL, the requirement to keep the reaction volume fluctuations at a minimum and the necessity to have sufficient statistics in each centrality bin. Volume fluctuations are relevant for ratios involving kaons, since their multiplicity does not strictly scale with the number of wounded nucleons  $N_W$ , or equivalently the reaction volume, in contrast to the multiplicity of pions

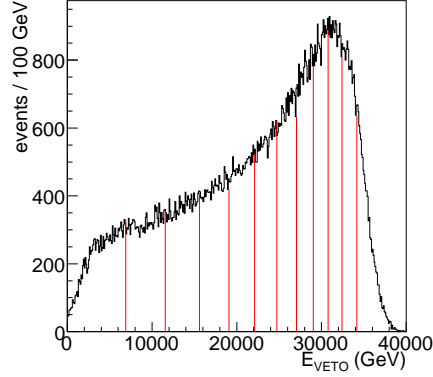


FIG. 2: (Color online) Distribution of the total energy  $E_{\text{VETO}}$  of the projectile spectators deposited in the VCAL of NA49 in Pb + Pb collisions at 158A GeV beam energy. An event vertex cut (see text) was applied to remove background triggers. Vertical lines separate bins of 5% of the total inelastic cross section.

and protons [19]. The influence of volume fluctuations on all particle-ratio fluctuations was studied by varying the centrality bin widths in the range from 3% - 20%. The results shown in Fig. 3 for the example of  $K/\pi$  ratio fluctuations in the most central collisions led us to choose 5% wide centrality bins, the smallest bin size that leaves sufficient statistics. For each bin the corresponding average number of wounded nucleons  $\langle N_{\text{W}} \rangle$  was obtained from the Glauber model approach using a simulation with the VENUS event generator [20, 21].

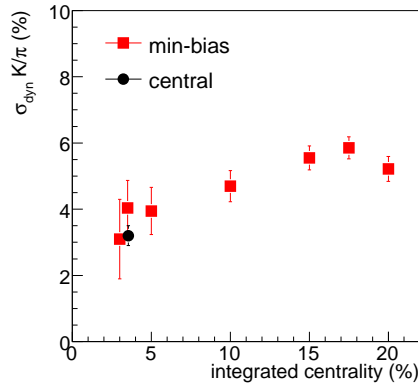


FIG. 3: (Color online) Dependence of the  $\sigma_{\text{dyn}}$  measure of  $K/\pi$  ratio fluctuations for the most central collisions on the width of the centrality bin in Pb+Pb collisions at 158A GeV.



### 3.3. Particle identification by $dE/dx$

The event-by-event measurement of particle ratios ideally implies track-by-track identification of the different particle types. The NA49 experiment provides energy loss measurements along the particle trajectories in the MTPCs with a resolution of approximately 4 % in the relativistic rise region for particle momenta  $p$  above 3 GeV/ $c$ . Since the separation of the  $dE/dx$  signals of pions, kaons, and protons at a given momentum is of the same order, track-by-track identification of particle types is not possible. Instead, we employ a statistical method, namely the Maximum Likelihood Method (MLM) to extract particle ratios from event-wise  $dE/dx$  distributions of negatively and of positively charged particles.

In a first step energy loss distributions of all accepted tracks in the event ensemble were constructed in bins of  $p$ ,  $p_T$  and  $\phi$ . The binning details are shown in Table II.

TABLE II: Binning in phase space used for fitting the inclusive  $dE/dx$  distributions. Due to overlap of the distributions for different particle species around momenta of 3 GeV/ $c$  the first 3 bins in total momentum were not used.

Variable	Range	$N_{\text{bins}}$	Bin size
$p$	1-120 GeV/ $c$	20	logarithmic
$p_T$	0-2 GeV/ $c$	10	0.2 GeV/ $c$
$\phi$	0- $2\pi$	8	$0.25\cdot\pi$
charge $q$	1,-1	2	-

The resulting inclusive specific energy loss distributions in each phase space bin were fitted with four Gaussian functions all having the same width for electrons, pions, kaons, and protons (and their antiparticles). The values of the nine fit parameters (eight positions and one width) define Probability Density Functions (PDF) for each phase space bin and were stored in a look-up table for later use in the event-by-event fits.

Using the PDFs one can calculate for each particle the four probabilities  $f_\alpha$  to be an electron (positron), a pion, a kaon or a proton (anti-proton). The sum of these probabilities weighted with coefficients  $\theta_\alpha$  become the factors in the likelihood function which depends on the coefficients  $\theta_\alpha$ :

$$L(\{\theta_\alpha\}) = \prod_{i=1}^N \sum_{\alpha} \theta_\alpha f_\alpha(q^i, p^i, p_t^i, \phi^i, (dE/dx)^i) , \quad (2)$$

where the index  $i$  runs over the  $N$  particles of the event. The coefficients  $\theta_\alpha$  are the relative yield fractions of each particle type in the event. The sum of the weights is constrained to unity:

$$\sum_{\alpha} \theta_\alpha = 1 . \quad (3)$$

By maximizing the likelihood function with respect to the relative yield fractions one obtains the best estimate of the different particle multiplicities in a given event. More details about the employed MLM can be found in [22].

### 3.4. Extraction of dynamical fluctuations

The fluctuations of particle ratios in the event ensemble are defined as the ratio of the root of the variance  $\sqrt{\text{Var}(A/B)}$  of the distribution of the event-wise particle yield ratio  $A/B$  to the mean  $\langle A/B \rangle$  of the same distribution:

$$\sigma = \frac{\sqrt{\text{Var}(A/B)}}{\langle A/B \rangle} . \quad (4)$$

Defined in this way  $\sigma_{\text{data}}$  will contain contributions from the finite number statistics, detector resolution, nonperfect particle identification and the genuine dynamical fluctuations. The first three contributions are considered as background. Since their contributions dominate the ratio fluctuation signal, their magnitudes have to be determined quantitatively. For an estimate of the statistical fluctuations and the detector resolution effects the event mixing method was applied. A new ensemble of artificial events was generated which contain particles from different real events, selected randomly such that in each artificial event no pair of particles originates from the same data event. In addition the multiplicity distribution of the mixed events was constructed to be the same as the corresponding distribution of the real events. By this token dynamical fluctuations, which may be present in data, are absent in the sample of mixed events. The measure  $\sigma_{\text{mix}}$ , evaluated according to Eq. 4 for the mixed events, contains thus only the background fluctuations. Examples of distributions

of the event-wise particle ratio for real and mixed events are shown in Fig. 4 for central and semi-peripheral Pb+Pb collisions.

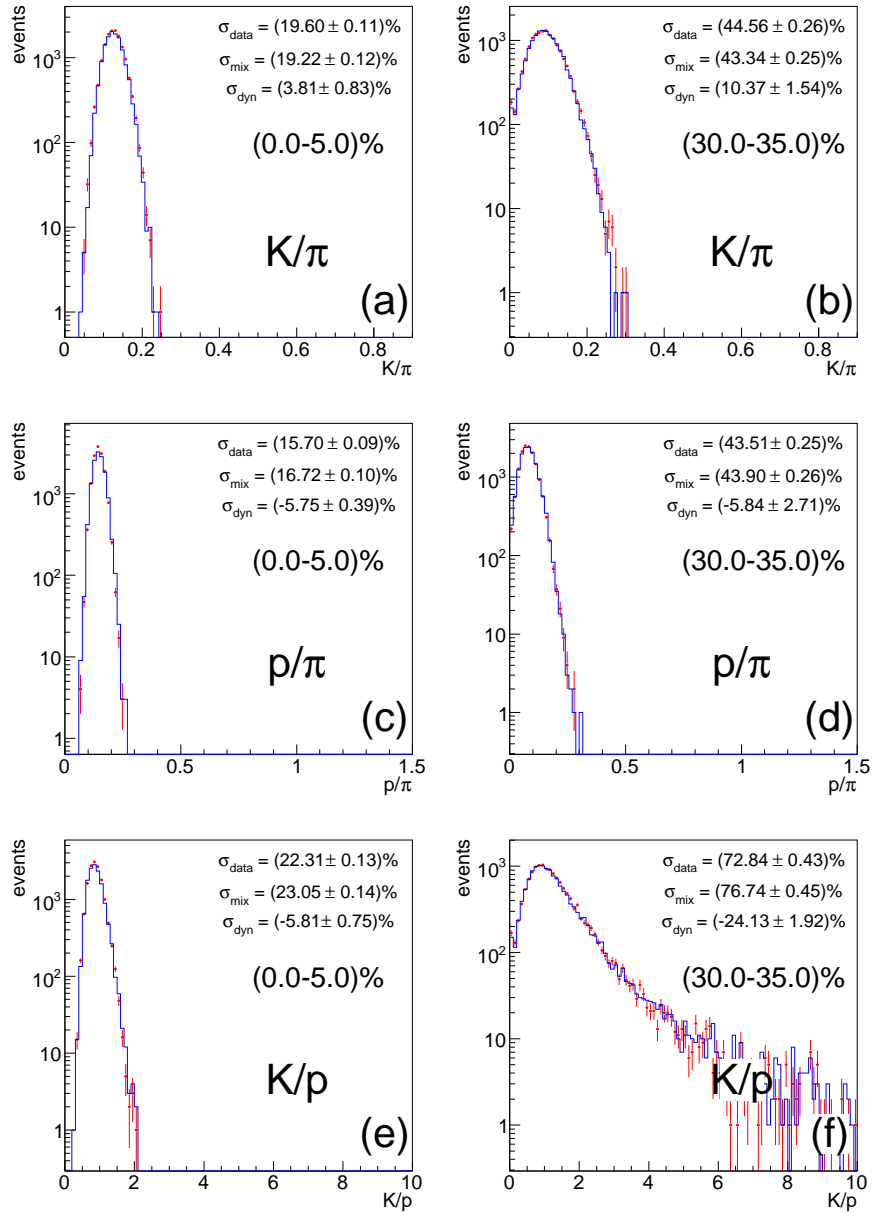


FIG. 4: (Color online) Event-by-event particle-ratio distributions for central (left) and semi-peripheral (right) in Pb+Pb collisions at 158A GeV. The data points show real event and the histogram mixed event distributions. Loose track cuts (see Table I) were applied.

We now define dynamical fluctuations ( $\sigma_{\text{dyn}}$ ) as the geometrical difference between the

fluctuations measured in real and mixed events:

$$\sigma_{\text{dyn}} = \text{sign}(\sigma_{\text{data}}^2 - \sigma_{\text{mix}}^2) \sqrt{|\sigma_{\text{data}}^2 - \sigma_{\text{mix}}^2|} . \quad (5)$$

Alternatively, the observable  $\nu_{\text{dyn}}$  [23], defined as:

$$\begin{aligned} \nu_{\text{dyn}} &= \nu - \nu_{\text{stat}} \\ \nu &= \frac{\text{Var}(A)}{\langle A \rangle^2} + \frac{\text{Var}(B)}{\langle B \rangle^2} - 2 \frac{\text{Cov}(A, B)}{\langle A \rangle \langle B \rangle} \end{aligned} \quad (6)$$

has been used to measure dynamical fluctuations of the particle ratio  $A/B$ . Here  $\nu_{\text{stat}} = 1/\langle A \rangle + 1/\langle B \rangle$  is the contribution from finite number statistics. Assuming that detector effects cancel in  $\sigma_{\text{dyn}}$  it was shown that  $\sigma_{\text{dyn}}$  is related [13, 14] to the fluctuation measure  $\nu_{\text{dyn}}$ :

$$\text{sign}(\sigma_{\text{dyn}}) \sigma_{\text{dyn}}^2 \approx \nu_{\text{dyn}} = \frac{\text{Var}(A) - \langle A \rangle}{\langle A \rangle^2} + \frac{\text{Var}(B) - \langle B \rangle}{\langle B \rangle^2} - 2 \frac{\text{Cov}(A, B)}{\langle A \rangle \langle B \rangle} . \quad (7)$$

For a check of the systematic uncertainties inherent in the mixed event background subtraction procedure we also determined  $\nu_{\text{dyn}}$  from our data. Owing to our non-perfect particle identification we again use mixed events to account for the background in the evaluation of  $\nu_{\text{dyn}}$  from the event-by-event fitted particle multiplicities:

$$\nu_{\text{dyn}} = \nu_{\text{data}} - \nu_{\text{mix}} . \quad (8)$$

The resulting values for  $\nu_{\text{dyn}}$  and  $\sigma_{\text{dyn}}^2$  were found to satisfy the equality of Eq. 7 within the systematic uncertainties estimated for  $\sigma_{\text{dyn}}$ .

As can be seen from Eqs. 5 and 7 the values of  $\sigma_{\text{dyn}}$  and  $\nu_{\text{dyn}}$  can be positive as well as negative. Assuming Poissonian single particle distributions, correlations lead to negative values of  $\sigma_{\text{dyn}}$ , while positive values are indicative of anticorrelations between the particles.

### 3.5. Systematic error estimation

In order to study the systematic uncertainties introduced by the track selection the results from the tight and loose sets of cuts (see Table I) were compared. We take the absolute difference between the results of the analysis with the two extreme conditions as an estimate of the corresponding systematic error.

Other sources of systematic uncertainty for the determination of the particle-ratio fluctuations are the  $dE/dx$  resolution and the method of event-by-event particle identification.

This systematic effect was studied with the help of simulated events from the UrQMD model [11]. In a first step the particles from the generated events were filtered by an acceptance table, representing the phase space bins of the real data which had sufficient statistics for successful fits of the  $dE/dx$  distribution. Then for each accepted track a  $dE/dx$  value was randomly generated from a parametrization of the inclusive  $dE/dx$  distribution for the true particle identity which depends on particle type and phase space bin. Finally, the accepted tracks with simulated  $dE/dx$  values were processed by the same analysis routines as the tracks from real data. In addition to the determination of particle multiplicities by the MLM the true particle identities as generated by the Monte Carlo code were stored. Figure 5 presents a comparison of the values of the dynamical particle-ratio fluctuations as obtained by using Monte Carlo identity and results from the  $dE/dx$  fit.

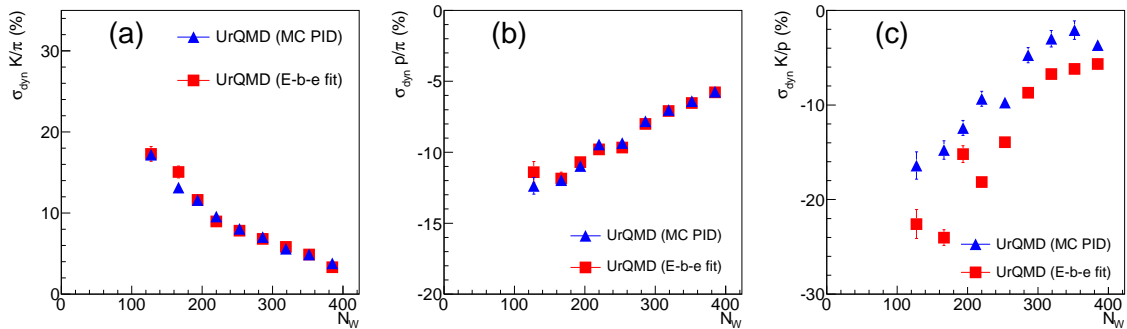


FIG. 5: (Color online) Centrality dependence of the measure  $\sigma_{dyn}$  for  $K/\pi$  (a),  $p/\pi$  (b) and  $K/p$  (c) ratio fluctuations evaluated for events simulated by the UrQMD model [11] using either true identity or the event-by-event fit results based on the simulated particle  $dE/dx$ .

The comparison of the results from both identification methods suggests the particle identification method based on the event-by-event MLM fit of the  $dE/dx$  distributions is valid in the  $\langle N_W \rangle$  range above 190. The difference observed for the  $K/p$  ratio was included in the systematic error.

## 4. EXPERIMENTAL RESULTS AND DISCUSSION

### 4.1. Centrality dependence of dynamical particle-ratio fluctuations

In this section we present our results on the centrality dependence of dynamical fluctuations of  $K/\pi$ ,  $p/\pi$ , and  $K/p$  ratios in Pb + Pb collisions at 158A GeV (numerical values are listed in Table III). The dot symbols in Fig. 6 show the dependence of  $\sigma_{\text{dyn}}$  (mean value of the results for tight and loose track cuts) of the three ratios on the average number of wounded nucleons  $\langle N_W \rangle$ . The systematic errors are indicated by the shaded bands. Also shown by square symbols are the values of dynamical fluctuations in central Pb + Pb collisions at 158A GeV beam energy from previous NA49 analyses [9, 10], which used a different event ensemble. The results from both analyses are in good agreement.

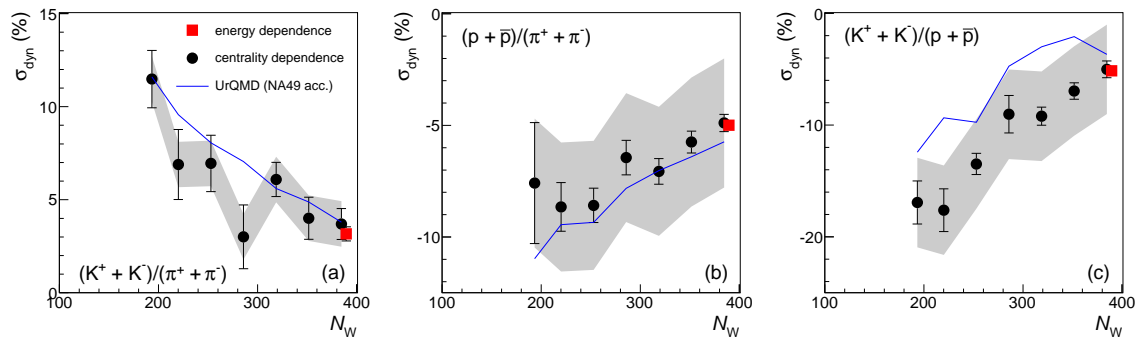


FIG. 6: (Color online) Centrality dependence of the measure  $\sigma_{\text{dyn}}$  of  $K/\pi$  (a),  $p/\pi$  (b), and  $K/p$  (c) ratio fluctuations. Dots show results from this analysis, squares show previously published measurements [9, 10]. The curves depict predictions of the UrQMD model [11] for the NA49 acceptance. The shaded bands show the systematic errors.

One observes the same trend for all considered particle ratios, namely that the absolute value of the dynamical fluctuations increases with decreasing centrality (decreasing  $N_W$ ). Interestingly, the UrQMD model [11] reproduces this behavior for all three ratios as demonstrated by the lines in Fig. 6. The model was previously found to fail in describing the energy dependence of  $\sigma_{\text{dyn}}(K/\pi)$  and  $\sigma_{\text{dyn}}(K/p)$  whereas it reproduced  $\sigma_{\text{dyn}}(p/\pi)$  [9, 10].

TABLE III: Numerical results for  $\sigma_{\text{dyn}}(\text{K}/\pi)$ ,  $\sigma_{\text{dyn}}(\text{p}/\pi)$ , and  $\sigma_{\text{dyn}}(\text{K}/\text{p})$  with statistical and systematic uncertainties for seven centrality intervals in Pb+Pb collisions at 158A GeV. Also listed are the corresponding average number of wounded nucleons  $\langle N_{\text{W}} \rangle$  and the average numbers of identified particles  $\langle \pi \rangle$ ,  $\langle \text{K} \rangle$ ,  $\langle \text{p} \rangle$  in the acceptance used for the analysis.

$\langle N_{\text{W}} \rangle$	$\sigma_{\text{dyn}}(\text{K}/\pi)$	$\sigma_{\text{dyn}}(\text{p}/\pi)$	$\sigma_{\text{dyn}}(\text{K}/\text{p})$	$\langle \pi^+ + \pi^- \rangle$	$\langle \text{K}^+ + \text{K}^- \rangle$	$\langle \text{p} + \bar{\text{p}} \rangle$
384	$3.7 \pm 0.8 \pm 1.2$	$-4.9 \pm 0.4 \pm 2.9$	$-5.0 \pm 0.7 \pm 4.0$	349.4	45.4	51.1
352	$4.0 \pm 1.1 \pm 1.2$	$-5.7 \pm 0.5 \pm 2.9$	$-7.0 \pm 0.7 \pm 4.0$	284.5	35.3	39.3
319	$6.1 \pm 0.9 \pm 1.2$	$-7.1 \pm 0.6 \pm 2.9$	$-9.2 \pm 0.8 \pm 4.0$	234.0	27.7	31.1
286	$3.0 \pm 1.7 \pm 1.2$	$-6.4 \pm 0.8 \pm 2.9$	$-9.0 \pm 1.7 \pm 4.0$	191.7	21.6	23.1
253	$7.0 \pm 1.5 \pm 1.2$	$-8.6 \pm 0.8 \pm 2.9$	$-13.5 \pm 0.9 \pm 4.0$	156.4	16.5	18.1
220	$6.9 \pm 1.9 \pm 1.2$	$-8.7 \pm 1.1 \pm 2.9$	$-17.6 \pm 1.9 \pm 4.0$	124.1	12.0	13.7
193	$11.5 \pm 1.5 \pm 1.2$	$-7.6 \pm 2.7 \pm 2.9$	$-16.9 \pm 1.9 \pm 4.0$	97.7	8.5	11.3

#### 4.2. Scaling behaviour of dynamical fluctuations

In this section we discuss various multiplicity scaling prescriptions which were proposed [13, 14, 24] with the aim of separating effects of changing average particle multiplicities from the energy and collision volume dependence of genuine dynamical fluctuations. It is important to note that for comparisons of experimental data with scaling calculations the measured multiplicities inside the experimental acceptances should be used. The analysis will be applied simultaneously to the centrality dependence reported in this paper and the energy dependence previously published in [9, 10].

In [13] it was shown that  $\sigma_{\text{dyn}}$  is expected to have a strong multiplicity dependence and might scale with  $\sqrt{1/\langle A \rangle + 1/\langle B \rangle}$ , where  $\langle A \rangle$  and  $\langle B \rangle$  are the average numbers of accepted particles of type A and B. As shown in Fig. 7(a,b) the measurements of the centrality and energy dependence of  $\text{K}/\pi$  and  $\text{p}/\pi$  fluctuations are consistent with the proposed scaling (sometimes called Poisson scaling). This result suggests that a large contribution to the observed variations appears to be caused by the changing multiplicities rather than by changes of the underlying correlations.

In contrast, the energy and centrality dependence of  $\text{K}/\text{p}$  ratio fluctuations, plotted in

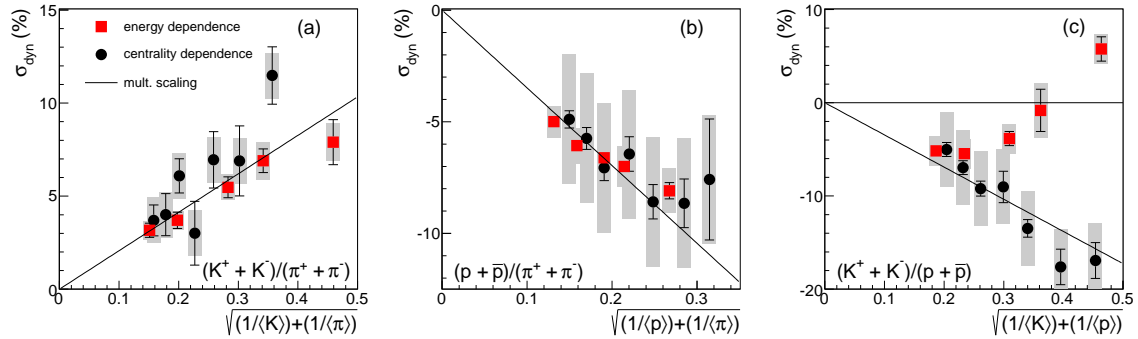


FIG. 7: (Color online) Dynamical fluctuations of the  $K/\pi$  (a),  $p/\pi$  (b), and  $K/p$  (c) ratio as a function of  $\sqrt{1/\langle K \rangle + 1/\langle \pi \rangle}$ ,  $\sqrt{1/\langle p \rangle + 1/\langle \pi \rangle}$ , and  $\sqrt{1/\langle K \rangle + 1/\langle p \rangle}$  respectively.  $\langle \pi \rangle$ ,  $\langle K \rangle$ , and  $\langle p \rangle$  are the average number of kaons and protons in the acceptance. The solid lines show fits to Poisson multiplicity scaling  $\sigma_{\text{dyn}} \propto \sqrt{1/\langle A \rangle + 1/\langle B \rangle}$  (see text). Shaded bands indicate systematic uncertainties.

Fig. 7(c) as a function of  $\sqrt{1/\langle K \rangle + 1/\langle p \rangle}$ , are not compatible with a common multiplicity scaling. The energy dependence shows a change of sign, indicating a change in the underlying correlation around 30A GeV beam energy. On the other hand, the centrality dependence exhibits a smooth decrease which is close to the Poisson multiplicity scaling behaviour (solid line in Fig. 7(c)).

As already mentioned in the introduction section the STAR collaboration has presented results on the collision energy dependence of particle-ratio fluctuations measured at RHIC in Au+Au collisions in terms of the observable  $\nu_{\text{dyn}}$ . First results for  $\sqrt{s_{NN}} = 7.7$  GeV [15] presented at conferences show a trend which differs from our results for  $K/\pi$  and  $K/p$  when compared using the relation between  $\nu_{\text{dyn}}$  and  $\sigma_{\text{dyn}}$  (see Eq. 7 in section 3.4). Intensive discussion could not yet determine the cause of the difference. However, we note that the acceptance in both rapidity  $y$  and transverse momentum  $p_T$  as well as selection of collision centrality are not the same.

Another scaling behaviour of the dynamical fluctuations of the  $p/\pi$  ratio was proposed in [16] based on the hypothesis that these originate from the production and decay of nucleon resonances. Such decays introduce correlations between  $p$  and  $\pi$ . Assuming that the variance terms in Eq. 7 can be neglected, the corresponding  $\sigma_{\text{dyn}}$  can be approximated by the following



equation:

$$\sigma_{\text{dyn}} \approx -\sqrt{\frac{\text{Cov}(A, B)}{\langle A \rangle \langle B \rangle}} \propto -\sqrt{\frac{(\langle A \rangle \langle B \rangle)^\alpha}{\langle A \rangle \langle B \rangle}}, \quad (9)$$

with the parameter  $\alpha$  expected to have the value 0.5.

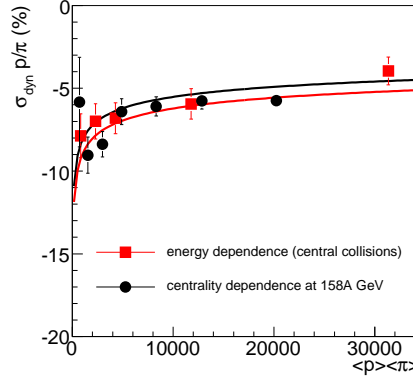


FIG. 8: (Color online) Dynamical fluctuations of the  $p/\pi$  ratio as a function of the product of average numbers of protons and pions in the detector acceptance.

The energy and centrality dependences of the dynamical fluctuations of the  $p/\pi$  ratio expressed as functions of the product  $\langle p \rangle \langle \pi \rangle$  are plotted in Fig. 8. A fit of the data points with Eq. 9 resulted in  $\alpha$  parameters equal to  $\alpha = 0.66 \pm 0.12$  for the energy dependence and  $\alpha = 0.51 \pm 0.03$  for the centrality dependence. This experimental observation supports the hypothesis that the source of the  $p/\pi$  ratio fluctuations is nucleon resonance production and decay.

An alternative scaling hypothesis was also investigated for the  $K/\pi$  ratio fluctuations. Since  $\langle K \rangle \ll \langle \pi \rangle$ , the dominating term in Eq. 7 for the dynamical fluctuations of the  $K/\pi$  ratio may be the kaon variance term, provided the covariance term can be neglected. Fig. 9 shows the energy and centrality dependence of the  $K/\pi$  ratio fluctuations versus the number of kaons  $\langle K \rangle$  in the acceptance. The curves in Fig. 9 indicate that also the function

$$f(\langle K \rangle) = a + \frac{b}{\langle K \rangle} \quad (10)$$

provides a good fit to both the centrality and energy dependence of  $K/\pi$  ratio fluctuations with  $a = 2.4 \pm 0.8$  and  $b = 62.1 \pm 16.6$ .

In the most peripheral collision events fewer phase space bins are useable because of the lower multiplicities. We repeated the analysis by restricting the extraction of  $\sigma_{\text{dyn}}$  to this

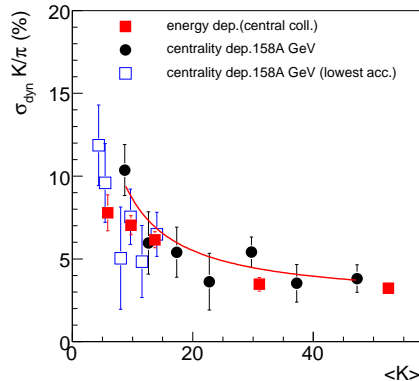


FIG. 9: (Color online) Dynamical fluctuations of the  $K/\pi$  ratio as a function of average number of kaons in the detector acceptance. Open square symbols show the results for the acceptance of the most peripheral set of events. The solid line shows the fit of the centrality dependence with the function of Eq. 10.

smaller acceptance for all centralities. The multiplicities  $\langle K \rangle$  in the restricted acceptance, of course, decrease. Nevertheless, the open square symbols in Fig. 9 demonstrate that the results for  $\sigma_{\text{dyn}}$  still follow the scaling of Eq. 10.

Presently the NA49 collaboration is in the process of developing and applying a new analysis procedure (identity method [25]) for the determination of event-by-event particle ratio fluctuations. It is designed to unfold the second moments of the multiplicity distributions of protons, kaons and pions. With this information, more direct tests of various models will become possible.

## 5. SUMMARY

We presented new measurements of the centrality dependence of  $p/\pi$ ,  $K/\pi$ , and  $K/p$  particle ratio fluctuations in terms of  $\sigma_{\text{dyn}}$  obtained by the NA49 experiment from Pb + Pb collisions at 158A GeV. The measure  $\sigma_{\text{dyn}}$  increases in absolute value with decreasing centrality for all these ratios. Comparisons to various multiplicity scaling schemes were made to both the centrality and the previously published energy dependences. Fluctuations of the  $p/\pi$  and  $K/\pi$  ratios are consistent with Poisson multiplicity scaling, thus suggesting that changing multiplicities rather than varying genuine correlations are the main source of these dependences. The  $p/\pi$  ratio fluctuations also scale with  $1/(\langle p \rangle \langle \pi \rangle)^{0.5}$ , supporting the

assumption that they originate from production and decay of nucleon resonances. The  $K/\pi$  ratio fluctuations are also compatible with a  $1/\langle K \rangle$  behavior, suggesting fluctuations of the kaon multiplicity as the main source of the measured energy and centrality dependences. In contrast, multiplicity scaling cannot describe the measurements of  $K/p$  fluctuations consistently. Although the centrality dependence of the absolute value of  $K/p$  ratio fluctuations exhibits a smooth increase for more peripheral collisions and is compatible with Poisson multiplicity scaling, a sign change is observed for the energy dependence. Therefore, the correlations causing  $K/p$  fluctuations appear to be changing in the SPS energy range.

## 6. ACKNOWLEDGEMENTS

Acknowledgements: This work was supported by the US Department of Energy Grant DE-FG03-97ER41020/A000, the Bundesministerium für Bildung und Forschung, Germany (06F 137), the Virtual Institute VI-146 of Helmholtz Gemeinschaft, Germany, the Polish Ministry of Science and Higher Education (1 P03B 006 30, 1 P03B 127 30, 0297/B/H03/2007/33, N N202 078735, N N202 078738, N N202 204638), the Hungarian Scientific Research Foundation (T032648, T032293, T043514), the Hungarian National Science Foundation, OTKA, (F034707), the Bulgarian National Science Fund (Ph-09/05), the Croatian Ministry of Science, Education and Sport (Project 098-0982887-2878) and Stichting FOM, the Netherlands.

- 
- [1] E. V. Shuryak, Nucl. Phys. A **702**, 83 (2002).
  - [2] N. Antoniou *et al.* (NA61 collaboration), CERN-SPSC-2006-034/P-330 and addenda.
  - [3] M. Aggarwal *et al.* (STAR collaboration), arXiv:1007.2613 (2010).
  - [4] F. Karsch, PoS **CPOD2007**, 026 (2007).
  - [5] M. Cheng *et al.*, Phys. Rev. D **79**, 074505 (2009).
  - [6] C. Schmidt, PoS **CPOD2009**, 024 (2009).
  - [7] T. Machado and N. Dupuis, Phys. Rev. E **82**, 041128 (2010).
  - [8] C. Alt *et al.* (NA49 collaboration), Phys. Rev. C **77**, 024903 (2008).
  - [9] C. Alt *et al.* (NA49 collaboration), Phys. Rev. C **79**, 044910 (2009).
  - [10] T. Anticic *et al.* (NA49 collaboration), Phys. Rev. C **83**, 061902(R) (2011).

- [11] S. Bass *et al.*, Prog. Part. Nucl. Phys. **41**, 255 (1998); M. Bleicher *et al.*, J. Phys. G **25**, 1859 (1999); UrQMD version 1.3 was used.
- [12] V. Konchakovski *et al.*, J. Phys. G **36**, 125106 (2009).
- [13] V. Koch and T. Schuster, Phys. Rev. C **81**, 034910 (2010).
- [14] B. Abelev *et al.* (STAR collaboration), Phys. Rev. Lett. **103**, 092301 (2009).
- [15] T. Tarnowsky (STAR collaboration), J. Phys. G **38**, 124054 (2011).
- [16] D. Kresan, PhD thesis Johann Wolfgang Goethe Universität Frankfurt am Main, 2010 (<https://edms.cern.ch/file/1179811/1/kresan-thesis.pdf>).
- [17] S. Afanasiev *et al.* (NA49 collaboration), Nucl. Instrum. Meth. A **430**, 210 (1999).
- [18] S. Wenig (NA49 collaboration), Nucl. Instrum. Meth. A **409**, 100 (1998).
- [19] NA49 collaboration, in preparation.
- [20] K. Werner, Z. Physik C **42**, 85 (1989).
- [21] Details can be found in: <https://edms.cern.ch/file/885329/1/vetocal2.pdf>.
- [22] C. Roland, PhD thesis Johann Wolfgang Goethe Universität Frankfurt am Main, 1999 (<https://edms/cern.ch/file/816020/1/rolandc.pdf>).
- [23] C. Pruneau, S. Gavin and S. Voloshin, Phys. Rev. C **66**, 044904 (2002).
- [24] S. Jeon and V. Koch, Phys. Rev. Lett. **83**, 5435 (1999).
- [25] M. Gazdzicki *et al.*, Phys. Rev. C **83**, 054907 (2011); M. Gorenstein, Phys. Rev. C **84**, 024902 (2011).